

Experimental Determination of J-integral at Elevated Temperatures

Ljubica Milović^{1,a}, Milorad Zrilić^{1,b}, Stojan Sedmak^{2,c}, Aleksandar Sedmak^{3,d}
and Meri Burzić^{4,e}

¹Faculty of Technology and Metallurgy, Karnegijeva 4, 11120 Beograd, Republic of Serbia

²Society for Structural Integrity and Life, Blv. vojvode Mišića 43, 11000 Beograd, Republic of Serbia

³Faculty of Mechanical Engineering, Kraljice Marije 16, 11120 Beograd, Republic of Serbia

⁴GOŠA Institute, Milana Rakića 35, 11000 Beograd, Republic of Serbia

^aacibulj@tmf.bg.ac.yu, ^bmisa@tmf.bg.ac.yu, ^csedmak@divk.org.yu, ^dasedmak@mas.bg.ac.yu,
^emerib@neobee.net

Keywords: steel P91, elevated temperatures, experimental determination of J integral, hardness, impact energy, microstructure

Abstract. In past two decades, the development of 9-12% Cr creep-resistant steel for critical components in coal-fired power stations that can withstand higher temperatures and pressures has been intensified in order to increase efficiency of supercritical plants. As the systems that can withstand ultra supercritical steam conditions are of an absolute necessity, it is an imperative to use the materials of adequate strength, physical properties and metallurgical stability at operating temperature. The aim is to prevent catastrophic failures arising based on a few mechanisms: leakage due to variation of the dimensions caused by creep, breakage-explosion due to fracture caused by stress and thermal fatigue due to cyclic stresses caused by heat.

Welding is the most important process of joining the components in such plants, and the heat-affected zone (HAZ) is often the weakest part of these structures. The variations of microstructures in HAZ affected by welding thermal cycle lead to inferior mechanical properties of this zone in comparison with base metal.

In present paper, the effect of post weld heat treatment (PWHT) on behaviour of welded structure made of material P91 at an operating temperature of 600°C has been presented. Research was conducted on the specimens with simulated HAZ, namely in critical zone in which the cracks of type IV might occur. The R curve for J-R curve testing was generated using the single specimen technique on the single edge side grooved test specimens. The tool for tensile testing used for putting the specimens into furnace was of special design.

Introduction

From thermodynamic point of view, fossil power plant efficiency can be increased if the inlet temperature and pressure are increased. Therefore, steels that can operate under such conditions have been developed all over the world [1, 2]. During seventies in OAK Ridge National Laboratory modified steel 9Cr-1Mo has been developed, leading to introduction and application of T91 steel for pressurized pipes and P91 steel for steamlines and collectors. These two steels replaced EM12 and X20CrMoV12-1 steels.

The microstructure of P/T91 steels is based on tempered martensite with stabilized carbides of $M_{23}C_6$ type with further strengthening due to solid solution of Mo and fine dispersion of carbonitride type (MX) rich with V and Nb.

In this paper the theoretical results [3-6], indicating the need for post weld heat treatment (PWHT) of steamline weldments, has been experimentally checked by testing the material for high stressed components in fossil power plants, operating under supercritical steam conditions (temperature 600°C, pressure 290 bar).

Having in mind the loading of a steamline, the heat-affected-zone (HAZ), as the most critical region in a weldment, has been tested by flat specimen tension, specimens from a notch region and cracked specimens. The base metal (BM) and simulated samples (SS) of new material have been tested in standard way regarding their composition and hardness, whereas the structure and microstructure, impact energy, tensile behaviour and fracture mechanics parameter have been tested at both the room temperature (20°C) and the operating temperature (600°C).

Material and Experimental Methods

Material and specimen design. The samples were taken from the pipe Ø320 mm, wall thickness 14 mm, length 140 mm, made of steel in P91 class [7,8], as indicated by its composition, table 1 [9].

Table 1 Chemical composition of tested material (percentage by mass)

C	Si	Mn	P	S	Cr	Ni	Cu	Al	Mo	As	V	Nb
0.120	0.289	0.396	0.009	0.002	8.04	0.080	0.082	0.024	0.850	0.007	0.242	0.073
W	Sb	Co	N	Ti	B							
0.013	0.0091	0.012	0.0400	0.003	0.0002							

Simulation of HAZ. In order to examine the influence of different welding thermal cycles on microstructure and mechanical properties of tested material, specimens with dimensions 11x11x70 mm, have been made using the thermal simulator SMITWELD. The characteristic transformation temperature in welding cycle, $A_{c1}=835^{\circ}\text{C}$ and $A_{c3}=930^{\circ}\text{C}$, have been determined using dilatometric curves, whereas the heat rate was 53.8 °C/s. During cooling the martensite started to form at temperature $M_s=375^{\circ}\text{C}$, whereas its transformation was completed at temperature $M_f=210^{\circ}\text{C}$. Before martensite transformation started small amount of bainite was formed.

Different regions in HAZ have been obtained by simulating one-pass welding with the following temperatures: 1386°C, 1300°C, from 1250°C and 950°C each 50°C, 925°C, 900°C and 850°C, with cooling time between 800°C and 500°C $t_{8/5}=40$ s. After welding, the specimens were PWHT at 730°C for 1 hour.

Fracture mechanics testing tools. Choice of specimens for J integral testing at 600°C depends primarily on available fracture mechanics testing tools. Two limiting factors existed: pipe wall thickness, limiting specimen thickness to 10 mm, and dimensions of the cylindrical high temperature-testing chamber (Ø70 x 320 mm). Thus the total length of a specimen, including fixing tool, Fig. 1, was limited to 250 mm, because of the grips of a special fork-like design, Fig. 2, and the ceramic seals.

Having in mind these limits, a SEN(T) specimen (Single Edge Notched Tension), has been used with B/W=5/10 mm. Specimen was made with treads M10 at both ends to match the fixing tool, Fig. 3. In order to avoid the problem of positioning the specimen into the chamber, a special joint connection at position 1 has been applied, Fig. 3. Such a tool construction has three articulated joints positioned at angle of 90°, so that loading conditions are enabled in a way that main stress direction directs crack tip opening. All tool parts are designed with minimum dimensions to enable efficient sealing of chamber with uniform temperature field and small heat loss.

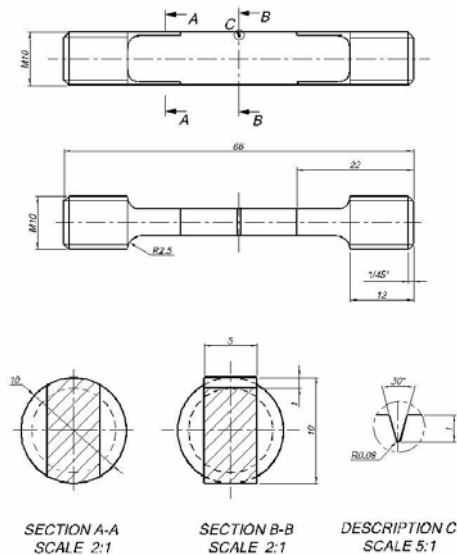


Figure 1. Specimen SEN(T) for J integral evaluation (dimensions are in mm)



Figure 2. High temperature chamber - upper tool fork, 1- tool body with sealing grooves, 2 - bolt retainer, 3 - hole for bolt without head

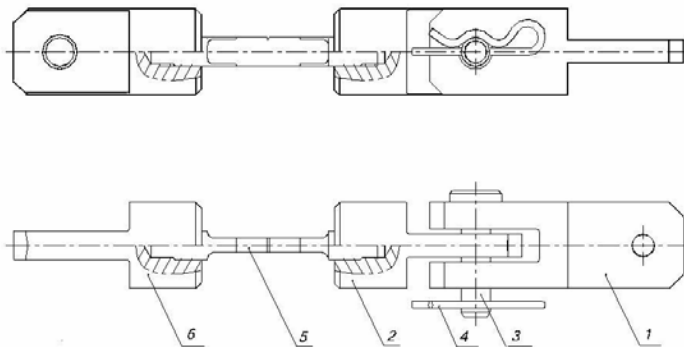


Figure 3. Tool and specimen for J integral evaluation (1-joint, 2-upper tension eye, 3-bolt with head and hole for hairpin, 4-hairpin, 5-specimen, 6-lower tension eye)

Calculation of total J_T integral for the notched specimen under plane stress tension. According to the recommendations [10], the total value of J_T integral for SEN(T) specimen can be calculated as:

$$J_T = J_e + J_p = \frac{K^2}{E'} + \frac{\eta(U_T - U_e)}{B_n(W - a_0)} \quad (1)$$

where $B=B_n$ denotes specimen thickness.

$$K = \sigma\sqrt{a} \cdot Y\left(\frac{a}{W}\right) = \frac{P}{BW} \cdot \sqrt{a} \cdot Y\left(\frac{a}{W}\right), \quad (2)$$

Where $Y(a/W)$ denotes geometry parameter, depending on crack length a and specimen width W ,
 P tensile load and $E'=E$ Young's elasticity modulus.

$$Y = \frac{\sqrt{\frac{2W}{a}} \operatorname{tg} \frac{\pi a}{2W} \cdot \left\{ 0.752 + 2.02 \left(\frac{a}{W} \right) + 0.37 \left(1 - \sin \left(\pi \frac{a}{W} \right) \right)^3 \right\}}{\cos \left(\frac{\pi a}{2W} \right)}, \quad (3)$$

Or

$$Y = \sqrt{\frac{W}{a}} \cdot \left\{ 1.4 \left(\frac{a}{W} \right)^{\frac{1}{2}} + 0.2556 \left(\frac{a}{W} \right)^{\frac{3}{2}} - 1.5 \left(\frac{a}{W} \right)^{\frac{5}{2}} + 2.42 \left(\frac{a}{W} \right)^{\frac{7}{2}} \right\}, \quad (4)$$

$$\eta^{LLD} = 5 \cdot \frac{a}{W} - 0.06 \text{ for } 1 \leq L/W \leq 3 \text{ and } 0.1 \leq a/W \leq 0.5, \quad (5)$$

i.e.

$$\eta^{CMOD} = 1 \text{ for } 1 \leq L/W \leq 4. \quad (6)$$

Results and Discussion

Hardness measurements. Hardness of BM and SS has been measured using Vickers method HV5 and HV1. Hardness was measured in the central part of simulated samples (at the surface opposites from the one where the thermal couple was fixed) at 5 points. The average value of BM hardness was 230 HV1, Fig. 4. The change of hardness of PWHT simulated samples with an increase of simulation temperature indicated somewhat reduced hardness at 925°C, verifying the choice of that specific temperature, made otherwise by the optical microscopy, as the testing temperature. More significant reduction of hardness value (close to 40 HV) is noticed for simulation temperature 850°C, just above AC_1 temperature. With an increase of the simulation temperature, the amount of ferrite that transform into austenite increases, reaching 90% at 925°C. At this temperature, there is

no significant dissolution of carbides and nitrides and thus any significant solid solution of carbon (C) and nitrogen (N) in the austenite. Therefore, the martensite formed during cooling has significantly lower content of C and N, causing limited segregation of $M_{23}C_6$ carbides and MX carbonitrides during PWHT and, consequently, the hardness lower than in the BM. Besides that, deposits of MX carbonitrides coarsen and coagulate, reducing their strengthening effect. Due to all aforementioned processes, the fine grain region in the HAZ, corresponding to simulation temperature 900°C-950°C, has the lowest hardness. With the increasing simulation temperature above 950 °C, the hardness increases because of the increased carbide solubility.

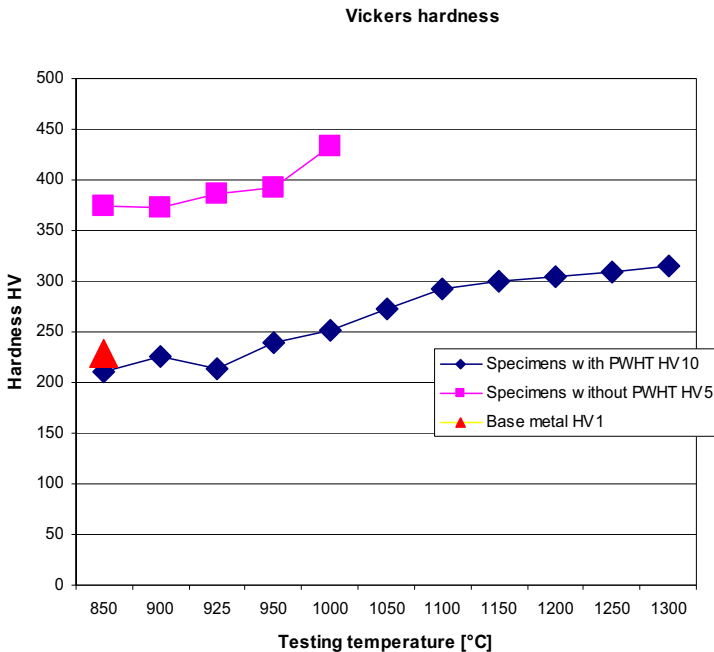


Figure 4 Results of Vickers hardness test measurements of simulated specimens and base metal

Tensile testing. Measured material properties are presented in table 2. For determination of yield strength $R_{p0.2}$ and ultimate strength R_m of BM and SS at 925°C with and without PWHT, at the room temperature (20°C) and the operating temperature (600°C), the smooth round bar specimen were used.

Table 2 Tensile properties of tested material

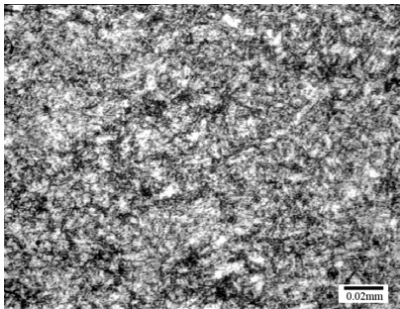
Tested material	Testing temperature T_p	Ultimate tensile stress	Tensile yield stress (0.2% offset)
	[°C]	R_m [MPa]	$R_{p0.2}$ [MPa]
BM	20	720,5	560
BM	600	313,5	231
925°C without PWHT	20	903	793
925°C without PWHT	600	498	407
925°C with PWHT	20	519	448
925°C with PWHT	600	363	295

Metallographic testing. By analysing the microstructure of all simulated samples, those heated up to maximum temperature 925°C have been pointed out as the most probable initiation sites for type IV creep cracking, Fig. 5 (optical Fig. 5a and scanning electron microscopy Fig. 5b). By using TEM, deposition of fine precipitates, as seen in Fig. 6 (c-d), appears at the grain boundary, as opposed to the precipitates inside the grain, Fig. 6 (a-b). This difference explains different behaviour under long-term high temperature loading, because deposition of fine precipitates at the grain boundaries improves the resistance of material to the creep cracking of type IV region. 925°C without PWHT, Fig. 6 (a-b) show that there are no precipitates on the grain boundaries so the resistance to plastic straightening at the grain boundaries is reduced that makes this state less convenient under creep conditions. In this way, the need for PWHT has been proved.

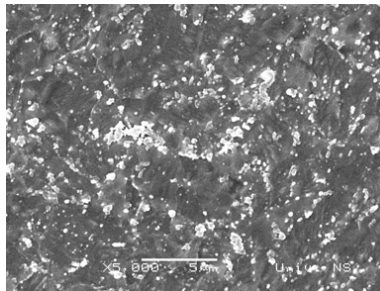
Impact testing. Impact testing has been performed on the instrumented pendulum, with standard specimens (EN 10045-1), with 2 mm V notch made on the side where thermo couple was fixed, both at room temperature and at operating temperature 600°C. Diagrams obtained from the instrumented pendulum have been used to evaluate maximum force, and energies for crack initiation and propagation, Fig. 7.

Impact toughness of the base metal at room temperature is $E=195.6$ J, with energy necessary for crack initiation and energy necessary for crack propagation $E_i=49.6$ J and $E_p=146$ J, respectively. At 20°C, the value of impact toughness of specimens simulated at 925°C with PWHT, is higher than impact toughness obtained at operating temperature of 600°C, where drop of strength and increase of plasticity occurred. For the samples simulated at 925°C, but without PWHT, a somewhat lower value of impact toughness was obtained in comparison with the samples with PWHT.

Fracture mechanics testing. The J integral has been evaluated both at room and at operating temperature using SEN(T) specimen, Fig. 8. As one can see, there is no significant difference in results for J-R curves for a material with and without PWHT.

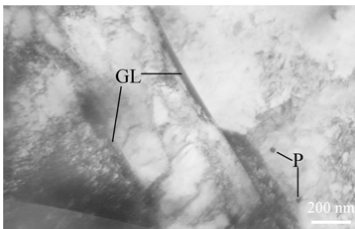


a) Microstructure of sample simulated at 925°C (VILELLA etching), light microscopy

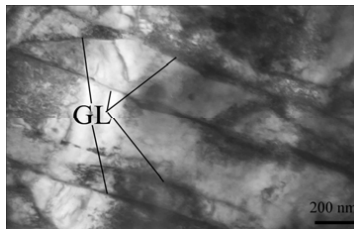


b) Microstructure of simulated samples, scanning electron microscopy (SEM)

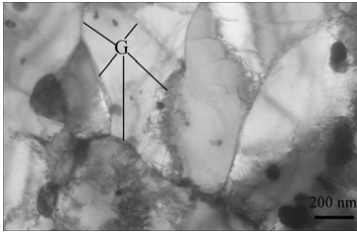
Figure 5 Microstructure of investigated material



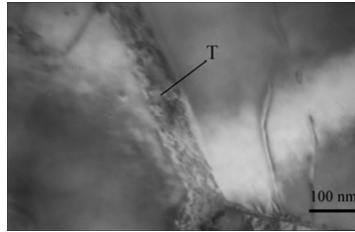
a) GL-lath boundaries P-precipitates



b) GL-lath boundaries



c) G-grain boundaries



d) T-precipitates

Figure 6 TEM Structure of sample simulated at 925°C without (a-b) and with PWHT (c-d)

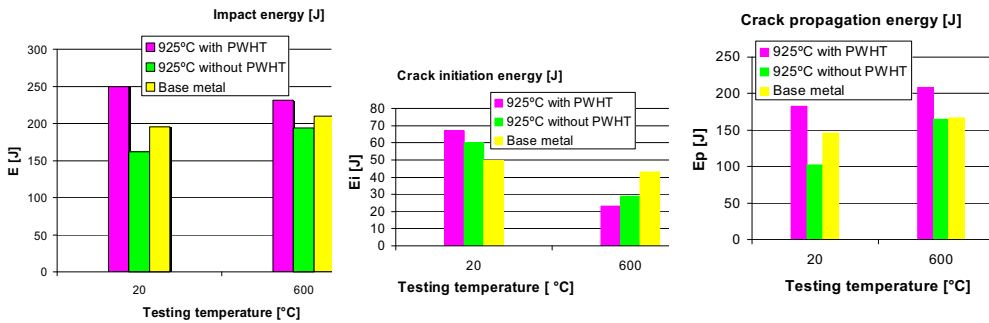


Figure 7 Comparison of total impact energy (a), crack initiation energy (b) and crack propagation energy (c) for BM and temperatures in HAZ 925°C with and without PWHT

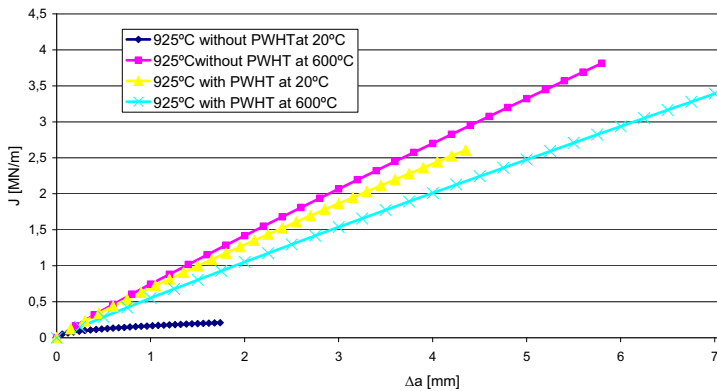


Figure 8 Comparison of resistance curves

Conclusions

Based on the results presented in the paper one can conclude the following:

- Fracture mechanics testing of material P91 has not indicated significant influence of PWHT on the crack resistance behaviour of the critical HAZ region (925°C);
- The impact testing have shown similar result – there is practically no difference in behaviour of the critical HAZ region (925°C) with and without PHWT;
- Other mechanical testing have shown expected behaviour for a material with and without PWHT – i.e. strength in the first case is reduced, whereas plasticity is increased;
- Only the TEM has indicated significant difference in microstructure of a material with and without PWHT, which explains their different behaviour under long-term high temperature loading, and proves the need of PWHT.

Having in mind the aim of this investigation, namely to experimentally determine the J-integral at elevated temperatures, one can notice that the appropriate measurement technique has been developed and applied. Similar technique can be applied for the long-term high temperature testing, including necessary modifications for different types of specimens and high temperature chambers.

References

- [1] H. Cerjak et al: Development and improvement of 9-12%Cr steels by a holistic R&D concept, Materials Science Forum Vols. 539-543 (2007), 2954-2959
- [2] P. J. Ennis: The mechanical properties and microstructures of 9% chromium steel P92 weldments, OMMI (Vol. 1, Issue 2) August 2002
- [3] K.-H. Schwalbe, U. Zerbst, W. Brocks, A. Cornec, J. Heerens, H. Amstutz: The ETM method for assessing the significance of crack-like defects in engineering structures, Fatigue & Fracture of Engineering Materials & Structures, Volume 21 Issue 10, October 1998, 1215-1231
- [4] K.-H. Schwalbe, B. K. Neale, J. Heerens: The GKSS test procedure for determining the fracture behaviour of materials: EFAM GTP 94, GKSS 94/E/60
- [5] B. Dogan, U. Ceyhan, B. Petrovski: Significance of creep crack initiation for defect assessment, IIW Journal, Issue: January/February 2006
- [6] B. Dogan: High temperature design approaches for welds, 2nd International Conference “Integrity of High Temperature Welds”, 10-12 November 2003, London, UK, 461-473
- [7] EN 10216-2: Seamless steel tubes for pressure purposes-Technical delivery conditions-Part 2: Non-alloy and alloy steel tubes with specified elevated temperature properties
- [8] ASTM A 335/A 335M-03, Standard Specification for Seamless Ferritic Alloy-Steel Pipe for High-Temperature Service, 2003.
- [9] Lj. Milović: The analysis of integrity of welded components of processing equipment for elevated operating temperatures, D.Sc. thesis, Faculty of Mechanical Engineering, University of Belgrade, 2008
- [10] ASTM E 1457-07: Standard Test Method for Measurement of Creep Crack Growth Times in Metals
- [11] Lj. Milović: Significance of cracks in the heat-affected-zone of steels for elevated temperature application, Structural Integrity and life, Vol. 8, No 1, pp. 41-50, 2008